Ultrahigh vacuum microscopy of the Si(111) boron $\sqrt{3}\times\sqrt{3}R30°$ surface

L. D Marks, R. Ai, S. Savage, and J. P. Zhang
Center for Surface Radiation Damage Studies, Department of Materials Science and Engineering, Northwestern University, Evanston, Illinois 60208

(Received 14 September 1992; accepted 9 January 1993)

The intensities of the diffraction spots for the boron induced $\sqrt{3}\times\sqrt{3}R30°$ Si(111) reconstruction in a bulk electron microscope sample examined in ultrahigh vacuum are compared with the results of multislice simulations. The intensities of the spots support the relaxed S5 model. We rule out the existence of any subsurface structure such as the stacking faults present in the Si(111) 7×7 surface.

I. INTRODUCTION

The importance of surfaces is well-known, but despite many years of study there are still many uncertainties. One of the reasons for this is that the surface structure has proved difficult in many cases to unambiguously determine experimentally. Until very recently the only techniques available utilized diffraction (scattering), and thus, were only able to quantitatively probe the average component of the surface; there are major problems for the inhomogeneous elements of the surface because of the phase problem. Scanning tunnel microscope (STM) has clearly produced a revolution in the quality and quantity of information available concerning surface structures but it does have one fundamental limitation; it is only sensitive to the very surface atoms (or more rigorously the surface density of states). For instance, STM was not able to fully decode the structure of the Si(111) 7×7 surface because the majority of the reconstruction was below the topmost layer.

Over the last few years, three techniques have risen to prominence for imaging surfaces in a conventional electron microscope: profile imaging where the surface is viewed edge on,[1–3] reflection electron microscopy or imaging reflection high-energy electron diffraction (RHEED),[4,5] and plan-view imaging where the electron beam is normal to the surface of interest.[6–8] Limited initially to a few surfaces with low sticking coefficients such as gold or some oxides, with the advent of ultrahigh vacuum (UHV) microscopes these techniques will play a larger role in the future. What electron microscopy can provide, complimentary to other surface science techniques is information simultaneously about both the surface and the bulk.

The intention of this note is to present data on the boron induced Si(111) $\sqrt{3}\times\sqrt{3}R30°$ reconstructed surface analyzed by UHV transmission electron microscopy, and compare the data with numerical simulations. The results are consistent with the relaxed S5 structure that has recently been proposed,[9–11] with fairly good agreement achieved between the experimental and calculated results, in particular the intensity of the {20} surface spots which are kinematically weak but can become strong in a dynamical condition. Furthermore, we can definitely rule out the presence of any additional subsurface features such as stacking faults.

II. EXPERIMENTAL METHOD

Boron-doped Si(111) samples were first cut into 3 mm disks, polished to a thickness of 200 μm and then dimpled to ~20 μm. These samples were then chemically polished until just electron transparent with a 10%HF/90%HNO_3 solution, then loaded into the side chamber of an UHV-H9000 high-resolution electron microscope[12] and baked for 1–2 days at ~200 °C. Substantial care was taken with the baking procedure to ensure that not only was the vacuum level after cooling in the low 10^{-10} to high 10^{-11} Torr range in the chamber, but also that during backfilling with argon to a pressure of $\sim 10^{-6}$ Torr, there was minimal ($<5\times10^{-10}$ Torr) degassing of hydrocarbons from the walls. The samples were then cycled through a 3 kV argon sputtering/annealing cycle using electron beam heating to ~800 °C until clean.

Analysis of the samples was conducted using the same microscope with direct UHV transfer of the specimen from the transfer chamber. The vacuum level in the microscope was 2×10^{-10} Torr, stable over a period of months both with and without the electron beam on. The primary techniques that will be of interest here are simple bright field and selected area diffraction, all of which were performed with the microscope operated at 300 kV.

Image simulations to analyze the details of the diffraction pattern were performed using the NUMIS software written by one of us (L.D.M.). These used the conventional multislice approach with 1.5 Å slices of the crystal along [111], with modifications to the top or bottom surface for the reconstruction. The simulations were performed both with and without an optical inelastic component of 0.05; rigor tests of the multislice procedure for surfaces[13] have demonstrated that this is the only important alteration to conventional multislice needed to simulate plan view surfaces.

III. RESULTS

We will very briefly describe some of the features of the microstructure during the cleaning process for reference. The initial surface, see Fig. 1(a), was contaminated with a 2–5 nm layer of partially graphitic carbon; this layer started as amorphous and partially graphitized during the bake. Ion beam sputtering led to a typical amorphous layer, see Fig. 1(b). By inference, we believe that this layer

 ©1993 American Vacuum Society

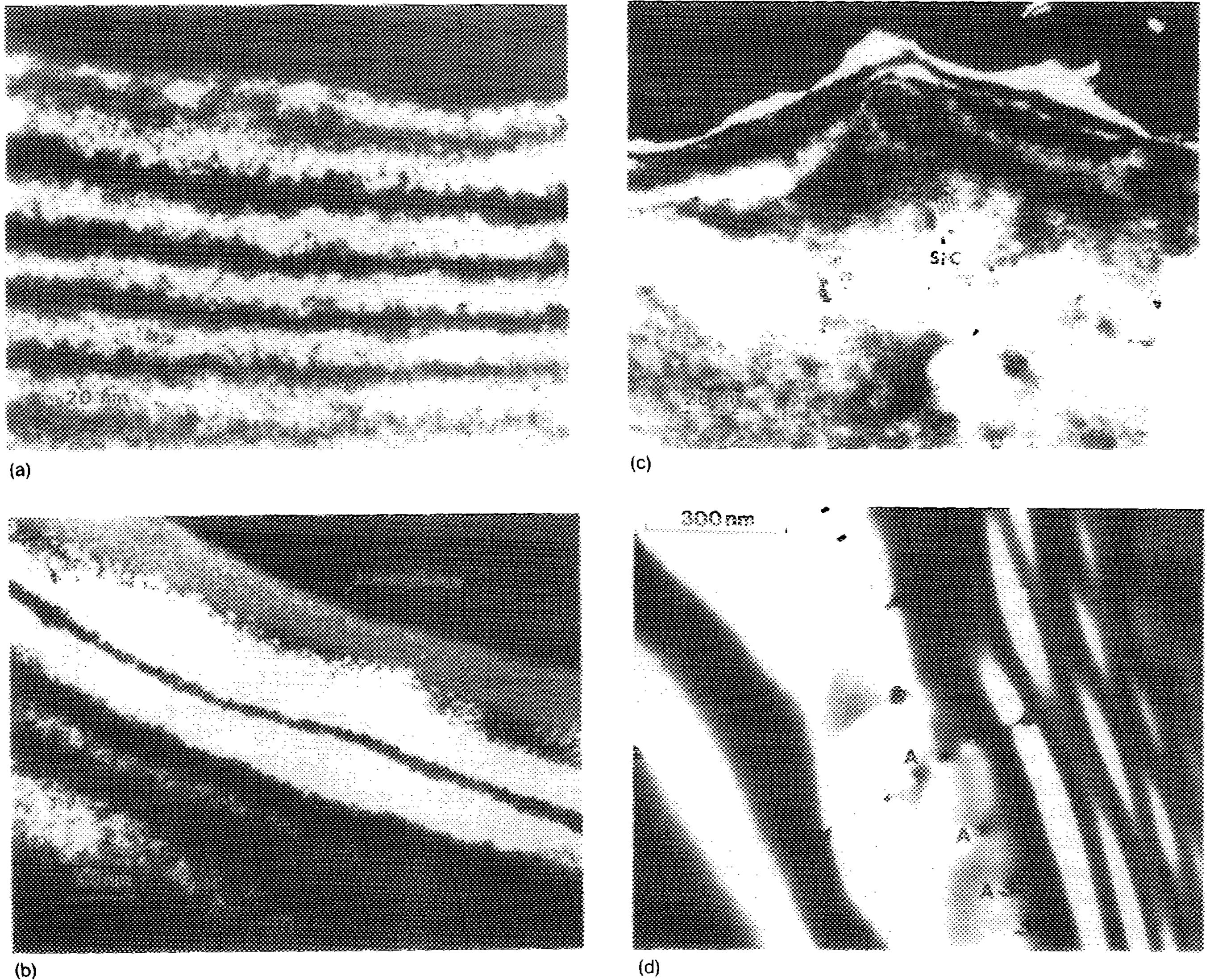

FIG. 1. Montage of the microstructure evolution of Si(111) during sample preparation: (a) initial surface after mechanical polish and chemical etch; (b) amorphization due to ion sputtering; (c) SiC islands marked by arrows formed during electron annealing; (d) clean surface obtained after ion sputtering and electron annealing. Screw dislocations are marked by A.

was a combination of silicon and carbon, the carbon content decreasing with increasing sputtering. The evidence for this is that in some cases annealing of the layer led to silicon carbide formation. Presumably, some of the surface carbon is being ion-beam mixed with the silicon. On annealing, the amorphous layer typically regrew epitaxially. If the carbon was not completely removed or the background hydrocarbon level was too high silicon carbide islands grew epitaxially, see the features marked by arrows in Fig. 1(c). With a clean enough sample, flat surfaces were obtained with some residual bulk defects such as screw dislocations labeled by "A" in Fig. 1(d).

The general features of the reconstructed surface are shown in the bright field image in Fig. 2 and the on and off the zone axis diffraction patterns in Figs. 3(a) and 3(b). The well annealed sample (see Fig. 2) showed a few voids left over from the ion-beam cleaning, and clear indications of surface steps marked by arrows. [The spot splitting in Fig. 3(a) and the extra spots in Fig. 3(b) are not reproducible. The spot splitting was not observed in the higher order diffraction spots and therefore, was not due to a long period surface reconstruction. There are many possible causes for these features. They could be due to strain, thickness variation, and dynamical diffraction.] In Fig. 3, a point of some importance that we will return to later is the intensities of the surface reconstruction spots. On the zone axis [Fig. 3(a)], all the surface diffraction spots are apparent with roughly equal (within an order of magnitude) intensities. Off the zone axis [Fig. 3(b)], the intensity of the (hk) spots was strongest when $|(hk)| = \sqrt{7}$, i.e., in a ring near to the bulk {220} diffraction spots, and the {20} spots were weak. Note as well that in Fig. 3(b) the signal-to-noise of the reconstructed diffraction spots is enhanced relative to the bulk background.

To analyze the intensity distribution, electron diffraction patterns were simulated for four models, although we will restrict presentation to only two of these. The models tested were as follows.

(a) A simple S5 reconstruction, see Fig. 4(a) with the

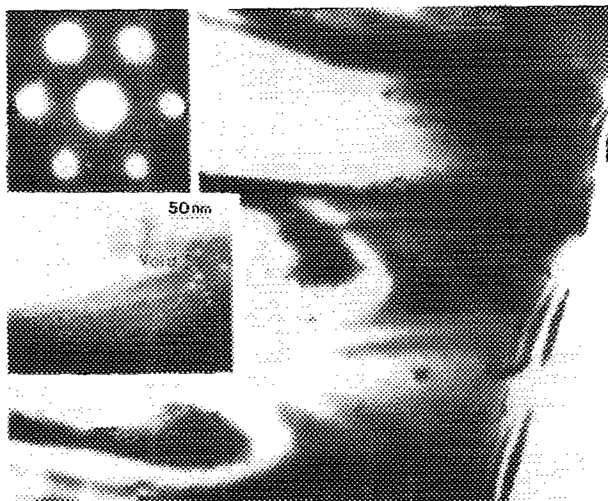

FIG. 2. A bright field image with diffraction pattern inset showing the reconstructed surface with steps marked by arrows. The steps can be seen more clearly in the higher magnification inset.

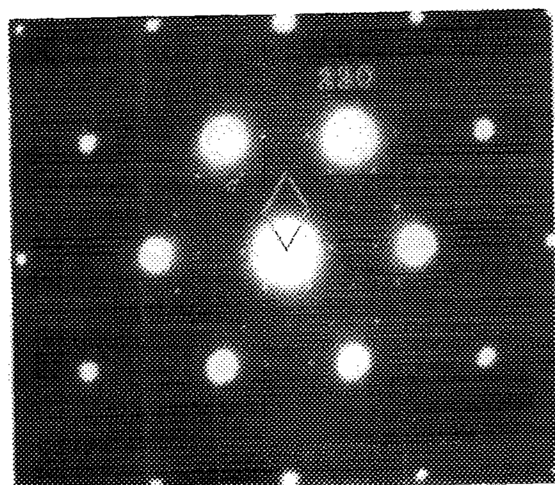

(a)

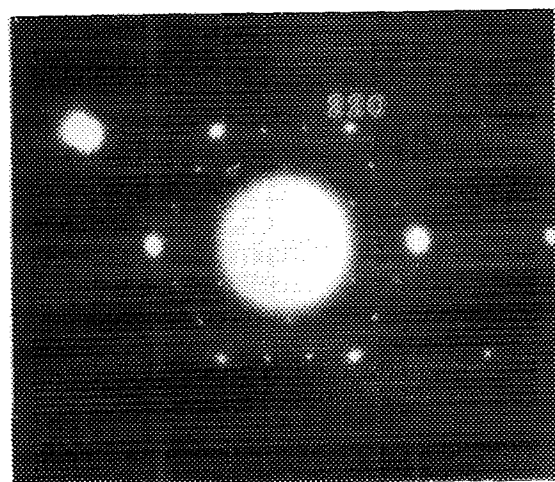

(b)

FIG. 3. Diffraction patterns taken from the reconstructed surface (a) on; (b) off zone axis.

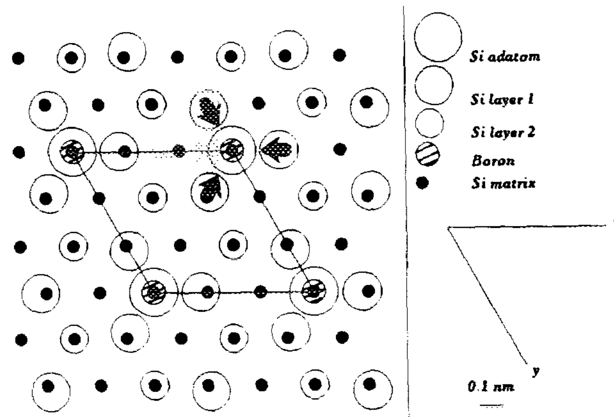

FIG. 4. Schematic illustration of the S5 model showing the in-plane change in position of the silicon atoms around the boron indicated by the arrows.

silicon atoms directly connected to the boron in pseudobulk sites.

(b) A relaxed S5 model using the atom position from Ref. 11.

(c) A rotated model with the S5 unit rotated 10°.

(d) A twinned model with the S5 unit rotated by 90°.

Although (c) and (d) have the same unit cells, the intensity distribution was not comparable with the experimental results.

The results of the analysis are summarized in the diffraction patterns shown in Figs. 5 and 6 and the graphs of the intensity of some of the beams versus specimen thickness shown in Fig. 7. Several points should be noted about this data.

(1) The intensity of the 1×1 spots are strongly damped by inelastic scattering, unlike the diffraction vectors except in very thin crystals, and their intensity is primarily determined by the bulk of the crystal.[13] The 1×1 spots will also be stronger in the calculations than in the experiments since the former refers to a perfectly ordered material and any sort of bulk or surface order will reduce the experimental intensity.

(2) In model (a), the intensity decays smoothly with increasing scattering angle since the Fourier coefficients of the reconstruction do the same. In contrast, the relaxed S5 model results are much more consistent with the experimental data, with an enhancement of the (hk) spots where $|(hk)| = \sqrt{7}$.

(3) The intensities calculated are semiquantitatively in agreement with the experimental results; in principle the agreement could probably be made quantitative with further work. In particular, one should note the weakness of the {20} spots in both the experimental and calculated off-axis diffraction patterns. In this context, it is important to recognize that transmission electron diffraction, unlike low-energy electron diffraction (LEED), is almost equally sensitive to subsurface layers as it is to the outermost surface layer. It, therefore, follows directly that we can rule

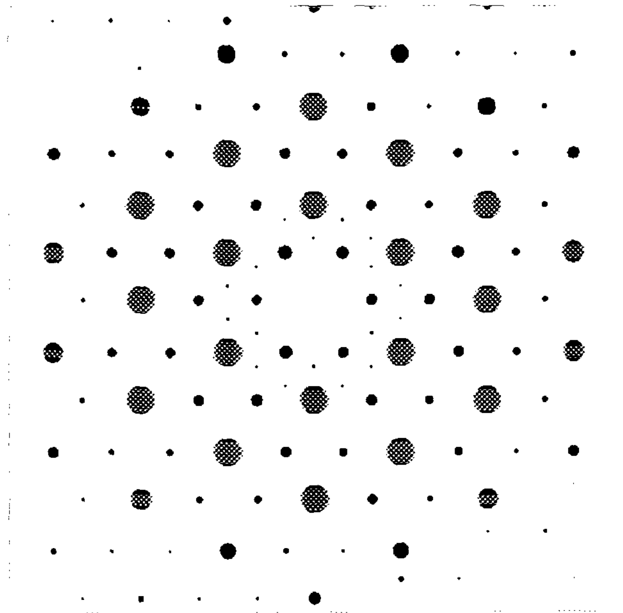

FIG. 5. Simulation of the diffraction pattern on the zone axis. The radius of the spots is proportional to the square root of the intensity of the diffracted beams in the multislice calculation. The intensity of the diffracted beams is scaled up by a factor of 10^5. If the radius is larger than 12 pixels, it is truncated. If the radius is smaller than 0.5 pixel, it is zero. Thickness = 156 Å; relaxation = 13.5%.

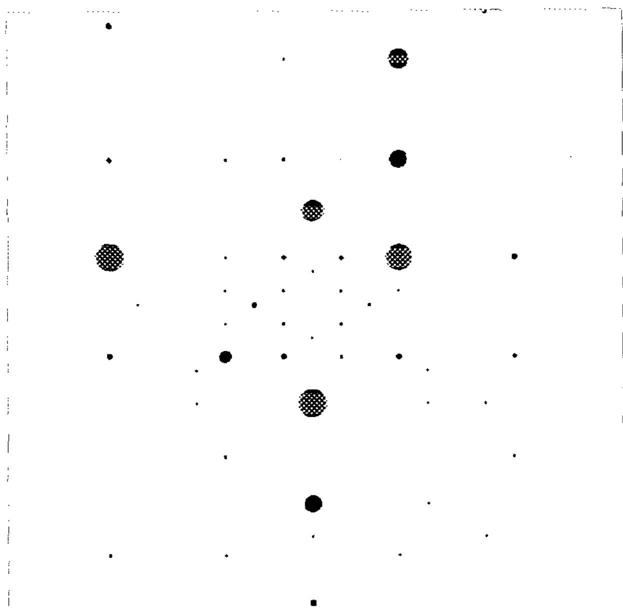

FIG. 6. Simulation of the diffraction pattern off the zone axis. The radius of the spots is proportional to the square root of the intensity of the diffracted beams in the multislice calculation. The intensity of the diffracted beams is scaled up by a factor of 10^5. If the radius is larger than 12 pixels, it is truncated. If the radius is smaller than 0.5 pixel, it is zero. The sample is tilted 112.0 mrad away from the zone axis; thickness = 156 Å; relaxation = 13.5%.

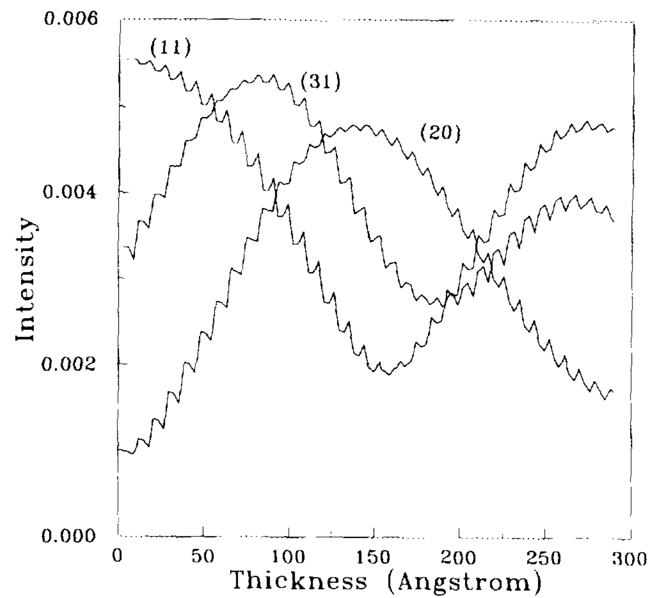

FIG. 7. The intensity of the surface spots and the reconstruction spots as a function of sample thickness on the zone axis. The optical inelastic component used in the simulation is 0.05.

out completely any substantive reordering below the surface in addition to the S5 element.

To be a little more precise, the intensity of the {20} reconstructed spots depends upon the in-plane relaxation of the silicon atoms towards the boron site. Shown in Fig. 8 is the ratio of the structure factors for {20} spots to the {31} spot as a function of this relaxation.

V. DISCUSSION

The results presented herein serve to strengthen the case for the S5 model for the boron (111) reconstruction. As

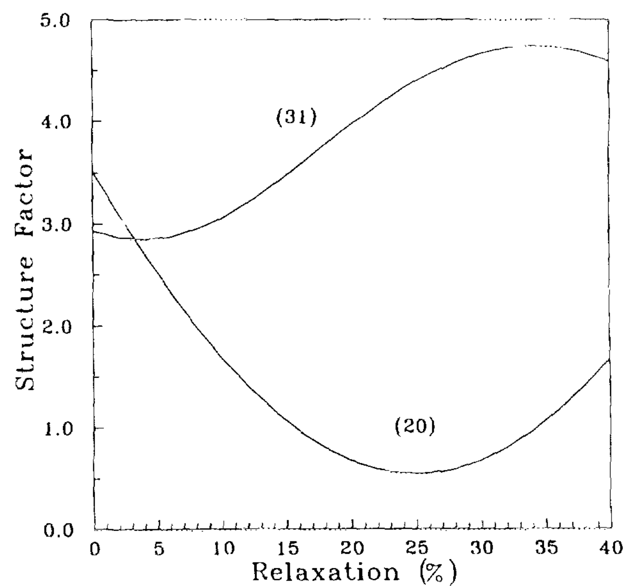

FIG. 8. The ratio of the structure factor for the {20} spots to the {31} spots as a function of relaxation.

mentioned above, the diffraction intensities could in principle be quantified and compared to experiment. However, this has already been done in some detail for LEED and x-ray data. The only piece of data that we can add to the story uniquely is to rule out any additional complications due to subsurface features which might be hidden from STM and LEED analyses.

ACKNOWLEDGMENTS

This work was supported by the Air Force Office of Scientific Research on Grant No. AFOSR 86-0344DEF. Funding for the UHV microscope was provided by the Keck Foundation, the National Science Foundation, and the Air Force Office of Scientific Research, and would have been impossible without the efforts of Robbie Kosak.

[1]L. D. Marks, Phys. Rev. Lett. **51**, 1000 (1983).
[2]L. D. Marks, in *Structure and Dynamics of Surfaces*, edited by W. Schommers and P. von Blackenhagen (Springer, Berlin, 1986).
[3]D. J. Smith, in *Chemistry and Physics of Solid Surfaces*, edited by R. Vanselow and R. Howie (Springer, Berlin, 1986).
[4]T. Hsu, S. Iijima, and J. M. Cowley, Surf. Sci. **137**, 552 (1984).
[5]N. Shimizu, Y. Tanishiro, K. Takanayagi, and K. Yagi, Ultramicroscopy **18**, 453 (1985).
[6]G. Nihoul, K. Abdelmoulas, and J. J. Metois, Ultramicroscopy **18**, 453 (1985).
[7]N. Ikarashi, K. Kobayashi, H. Koike, H. Hasekura, and K. Yagi, Ultramicroscopy **26**, 195 (1988).
[8]J. M. Gibson, in *Surface and Interface Characterization by Electron Optical Methods*, edited by A. Howie and U. Valdre (Plenum, London, 1988).
[9]I. W. Lyo, E. Kaxiras, and Ph. Avouris, Phys. Rev. Lett. **63**, 1267 (1989).
[10]R. L. Headrick, I. K. Robinson, E. Vlieg, and L. C. Feldman, Phys. Rev. Lett. **63**, 1253 (1989).
[11]P. Bedrossran, R. D. Meade, K. Mortensen, D. M. Chen, J. A. Golovchenko, and D. Vanderbilt, Phys. Rev. Lett. **63**, 1257 (1989).
[12]R. Ai, M. I. Buckett, D. Dunn, T. S. Savage, J. P. Zhang, and L. D. Marks, Ultramicroscopy **39**, 387 (1991).
[13]L. D. Marks, T. S. Savage, J. P. Zhang, and R. Ai, Ultramicroscopy **38**, 343 (1991).